22nd Australasian Fluid Mechanics Conference AFMC2020
Brisbane, Australia, 6–10 December 2020
DOI: 10.14264/uql.2020.xxYY

Numerical simulation of a two-stage contra-rotating vertical axis wind turbine

B. Ko[1], S. Liu[1], Z. Fang[1], Y. Ahmudiarto[2], B. Nugroho[1] and C. Chin[3]

[1] Department of Mechanical Engineering
University of Melbourne, Melbourne, Victoria, 3010, Australia

[2] Research Center for Electrical and Mechatronics
Indonesian Institute of Sciences, Bandung, West Java, 40135, Indonesia

[3] School of Mechanical Engineering
University of Adelaide, Adelaide, South Australia, 5005, Australia

Abstract

This study presents a three-dimensional computational fluid dynamics investigation of the Vertical Axis Wind Turbine (VAWT) with a contra-rotating arrangement. Here we investigate the performance of the contra-rotating VAWT by varying two different parameters, namely the airfoil profile (thickness and camber size), and the vertical distance between the top and bottom rotor. Preliminary data indicate that thicker airfoils generate a higher coefficient of power (C_p) than the thinner airfoils. The cambered airfoils, however, do not generate such a trend, this suggests that cambered airfoil rotors may generate wingtip vortices that influence the opposite rotors. The wingtip vortex may also influence the turbine's C_p when both rotors are moved closer and further. Our simulations show that symmetrical airfoils would generate higher C_p when the upper and lower rotors are close to each other. However, this is may not necessarily the case for the cambered airfoil.

Keywords
Vertical Axis Wind Turbine (VAWT); H-Darrieus type VAWT; RANS CFD; Contra-rotating VAWT; Blade Profile Design.

Introduction

In the past few decades, the concept of Vertical Axis Wind Turbine (VAWT) has attracted considerable attention especially in regions where the wind direction is constantly changing and the wind speed is relatively low. Compared to the more common Horizontal Axis Wind Turbine (HAWT), VAWT is characterised by its ability to change its rotation direction (based on the wind source direction), the absence of a yawing mechanism, ease of installation, and low maintenance cost [2]. One of the most common VAWTs is the Darrieus type, which is a lift-driven VAWT with high potential performance, and its simplest form is known as the H-Darrieus (straight-bladed) [1, 2]. Unlike the other Darrieus type wind turbine, the H-Darrieus wind turbine only uses simple 2-Dimensional airfoil to generate lift, which would lead to a simpler design and less manufacturing cost. Such an advantage makes H-Darrieus type wind turbine an ideal power generation system for remote and underdeveloped areas or communities that have inconsistent wind direction and speed.

Although it has plenty of advantages, the Achilles' heel of VAWT wind turbines is that they are less efficient than HAWT. Due to their airfoil and rotor design, not all of VAWT airfoil experience wind loading simultaneously: only the incoming-wind faced airfoil generates force to rotate the motor while the rest do not. One way to improve the efficiency of VAWT is to combine two or more VAWT in the vertical direction to create a contra-rotating wind turbine [3, 4]. A recent report by Didane et. al [3] shows that one could build a simple H-Darrieus contra-rotating wind turbine with just a regular generator and without the need to use two contra-rotating shaft or a contra rotating generator. Following their experimental work, Didane et. al [4] conducted computational fluid dynamics (CFD) studies to analyse the influence of airfoil aspect ratio and the axial distance between the two rotors on the wind turbine's power coefficient. Their report shows that shorter distance between rotors and large airfoil aspect ratio generate the highest amount of power.

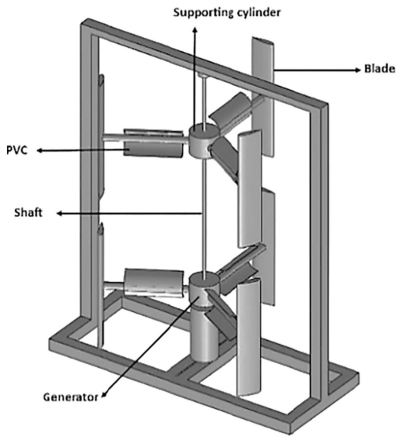

Figure 1. Illustration of H-Darrieus contra-rotating vertical axis wind turbine (taken from Didane et. al [4])

Despite their potential, there have been limited new studies on H-Darrieus contra-rotating wind turbine. Particularly on other important parameters such as different airfoil type, blade design, etc. In this report, we extend the CFD study of Didane et. al [4] by conducting a Reynolds-Averaged Navier-Stokes (RANS) CFD on H-Darrieus contra-rotating wind turbine. Here we will investigate the influence of the axial distance between the top and bottom rotors in more detail, as well as the airfoil thickness and camber size.

H-Darrieus contra-rotating wind turbine design and configuration

The wind turbine model is based on the design of Didane et. al [3, 4]. Here two sets of three blades/airfoils H-Darrieus contra-rotating wind turbine are designed in a vertical configuration (see Figure 2). Structure details such as struts and shaft are neglected, which aids in reducing the complexity of the simulation setup, moreover, their dimension and cross-section area is relatively small compared to the airfoils. Note that here we also do not include the PVC pipe, in which which they added to start the turbine. The reason for not including the PVC is that we intend to see how the turbine behaves when it is at its most basic configuration.

The wind turbine's design parameters and dimensions are tabulated in Table 1. The dimension was chosen to fit the maximum

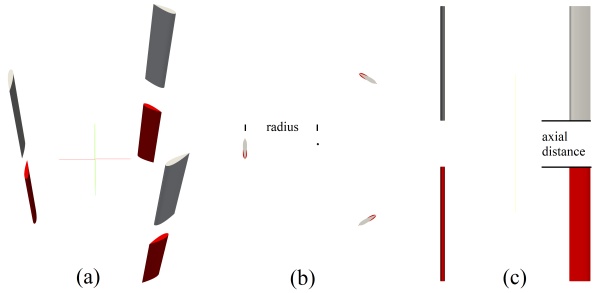

Figure 2. Geometric 3-dimensional configuration model of H-Darrieus contra-rotating wind turbine with:(a) orthogonal (b) top and (c) front views

allowable dimension of the available wind tunnel for possible future experiments and to closely match the studies of Didane et. al [3, 4]. In this study we will vary three different parameters namely: rotor axial distances, airfoil thickness, and airfoil camber size (see Table 2 for details). Both of the thickness and camber size airfoils are based on the NACA designed airfoil. The NACA airfoil is characterised with four digit code where the first digit describes the maximum camber as a percent of the chord, the second digit describes the position of the maximum camber from the airfoil leading edge in tenths of the chord, and the last two digits characterise the maximum thickness of the airfoil as a percent of the chord.

Parameters	Specification
Turbine type	Darrieus Type VAWT
Blade shape	Straight Blades
Cross-sectional shape	NACA 4-digit Blades
Number of blades, n	3
Rotor/Turbine diameter, d (mm)	800
Rotor/Turbine height, h (mm)	500
Chord length, c (mm)	100

Table 1. Fixed parameters of the H-Darrieus contra-rotating wind turbine

For the different airfoil thickness, we employ NACA0005 to NACA0025 with an increment of 5 for the last two digits, implying an increase of 5% in the maximum thickness of the airfoil as a percent of the chord. Figure 3(a) illustrates the NACA0015, which implies that the maximum thickness of the airfoil is 15% percent of the chord. For the different camber cases (i.e. Figure 3b), all of the airfoils have an identical thickness of 15% of the chord (hence the last two digits of NACA2415 - NACA6415).

Topic	Thickness
Blades (NACA)	0005; 0010; 0015; 0020; 0025
Topic	Camber Size
Blades (NACA)	2415; 3415; 4415; 5415; 6415
Topic	Axial Distance
Distance (mm)	50; 100; 150; 200; 400

Table 2. Simulation parameter cases.

Note that for the varied camber size cases, we have conducted several initial tests where we compare the effect of the orientation of the cambered blades, i.e. convex side facing inwards and the concave side facing outwards. After several initial tests with NACA4415, it is observed that the outward-facing airfoils outperforms the inward-facing airfoils for all wind speed. Hence in this report, all cambered airfoil simulations are facing outwards.

Simulation setting

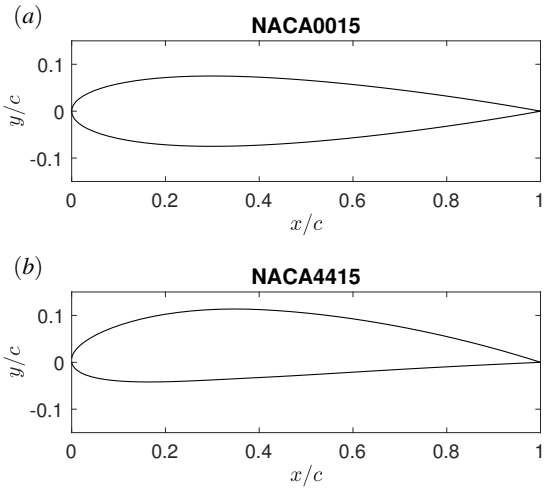

Figure 3. Illustration of NACA airfoil 0015 (a) and 4415 (b). Both airfoils have a similar thickness of 15% percent of the chord.

We conduct the H-Darrieus contra-rotating wind turbine simulation using an open-source computational fluid dynamics (CFD) solver OpenFoam on The University of Melbourne's Spartan HPC (High Performance Computing) system. Here we use the $k-\omega$ Shear Stress Transport (SST) as the turbulence model as it has been known to work well with H-Darrieus wind turbine [4] .

Computational domain

The computational domain consists of two parts: the stationary domain and rotation domain (see Figure 4). The rotation domain, which is denoted by red is further subdivided into two, namely: the top and bottom rotating zone due to different rotating directions. The stationary domain is composed of six surfaces: a velocity inlet, which simulates the wind inflow, and a pressure outlet, which simulates the atmospheric exit, along the x-axis; a no-slip wall (ground) at the bottom (negative y-direction) and three slip walls for other side surfaces. Each rotating zone has a turbine boundary which is defined as a no-slip wall. The rotating domain radius R (750 mm) is defined as $1.875r$ where r is the turbine/rotor radius (400 mm), and its height H is defined as $4h$, where h is 500 mm. The rotational speed is applied to cells in each rotating zone.

The computational domain size is 32R $\times$ 12R $\times$ 12R in the streamwise, spanwise and wall-normal direction respectively. The stationary domain is discretised to achieve an average mesh resolution of 0.5 m. The rotating domain is discretised to achieve an average mesh resolution of 0.03125 m. The grid resolution of the region around the turbine blades is further refined to an average mesh resolution of 0.0019 m. The total number of grid points for the simulation is approximately 1.5 Million. This number of grid number is chosen after a grid independence analysis, whereby the current grid resolution ensures the residuals to fall in the range of between 10^{-4} to 10^{-5}. As the grid resolution is not sufficient to resolve the boundary layer on the wind turbine blades, which is typical for RANS simulations, a wall-function is applied in the near-wall region, which is a blended function of the viscous and logarithmic laws.

Boundary conditions

In this study, for all simulation parameter cases (i.e. different axial distance, airfoil thickness, and airfoil camber size) we used a range of wind speed from 5 m/s to 12 m/s with 1 m/s increments (8 wind speeds in total). Air properties used in the simulations are based on $T = 25°C$, where kinematic viscosity

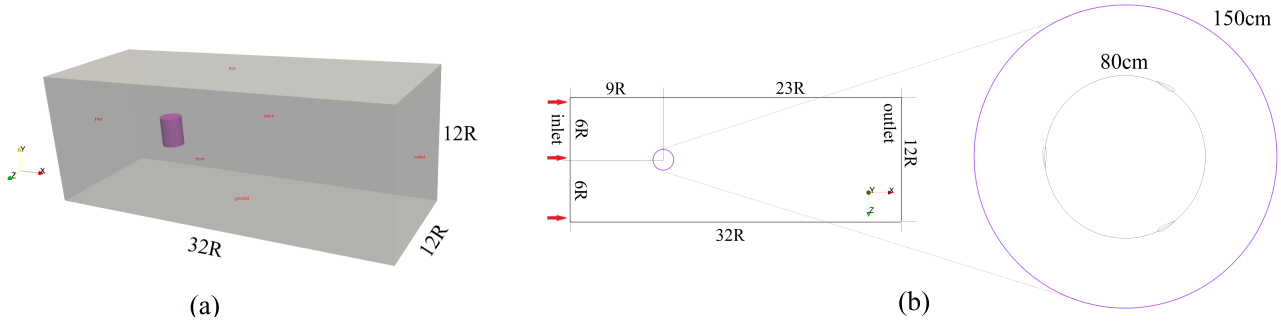

Figure 4. Simulation domain in (a) orthogonal view and (b) top view. Red region in (a) denotes rotating domain and the grey is stationary domain.

$\nu = 1.562 \times 10^{-5}$ m^2/s and density $\rho = 1.184$ kg/m^3. Table 3 lists the wind speed and the wind turbine's associated revolution per minute (RPM) and tip speed ratio (TSR). The tip speed ratio is of vital importance in any VAWT design, it represents the turbine's rotating speed with respect to the wind speed:

$$\text{TSR} = \lambda = \frac{\nu}{U} = \frac{\omega r}{U}, \tag{1}$$

where ω is the rotational speed in rad/s of the turbine, and U is the wind speed in m/s. Generally, high TSR is desirable for the operation of an electrical generator, while low TSR values may lead to low efficiency as wind passes through the gaps between the blades.

Wind Speed m/s	Top Rotor clockwise		Bottom Rotor anti-clockwise	
	RPM	TSR	RPM	TSR
5	45	0.38	56	0.47
6	48	0.34	72	0.50
7	60	0.36	81	0.48
8	70	0.37	98	0.51
9	82	0.38	115	0.54
10	87	0.36	130	0.54
11	96	0.37	144	0.55
12	112	0.39	158	0.55

Table 3. RPM and TSR for each wind speed, adapted from Didane et al. [4]

Performance of the contra-rotating wind turbine

Through out this report, the performance of the contra-rotating wind turbine will be characterised via coefficient of power C_p :

$$C_p = \frac{P_{out}}{P_{in}} = \frac{\tau\omega}{\frac{1}{2}\rho_{air}AU^3} = \frac{\omega d}{2U}\frac{\tau}{\frac{1}{4}\rho_{air}AdU^2} \tag{2}$$

where τ is the torque, d is the diameter, A is the swept area equals to dh, with h being the height, and ρ_{air} is the air density. The C_p provides a dimensionless measurement of the mechanical efficiency of the H-Darrieus contra-rotating wind turbine configuration, which allows direct comparison between the three-parameter configurations. The C_p is calculated based on the torque simulated with wind speed ranging from 5 m/s to 12 m/s. Note that through out the rest of the report, the coefficient of power described is taken as the average of the top and bottom turbine's C_p.

Results

Influence of different airfoil thickness

The first parameter analysed is the airfoil thickness, here all of the airfoils have a similar cross-section both on the lower and upper surface (teardrop shape, see Figure 3a). The distance between the upper and lower rotor is 0.2 m for all airfoil thickness. Figure 5 shows the plot of C_p versus wind speed for NACA0005 - NACA0025. The plot clearly shows an increase in C_p with airfoil thickness, with NACA0025 outperforming the other thinner airfoils.

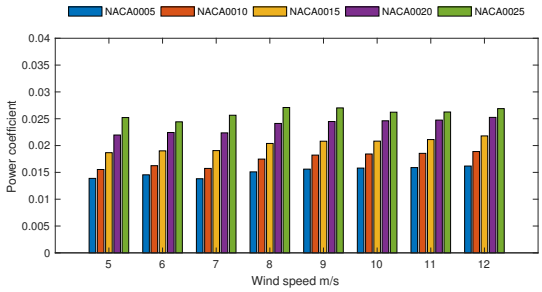

Figure 5. Power coefficients at a various wind speeds for different airfoil thickness.

Influence of different airfoil camber

Figure 6 shows the plot of C_p versus wind speed for different airfoil cambers. For this parameter, the axial distance (i.e. the distance between the top and bottom rotor) chosen is 0.2 m, which is similar to the airfoil thickness variation case. The plot shows that as we increase the camber size from NACA2415 to NACA5415, the C_p decreases with wind speed. However, for NACA6415, the C_p is consistently higher than the other cambered airfoil cases for all wind speeds. The sudden increase of the performance in C_p of the NACA6415 is difficult to explain and more analysis is needed. However, we believe that it may be due to the wingtip vortex from both the top and bottom rotors that influence the opposite rotors.

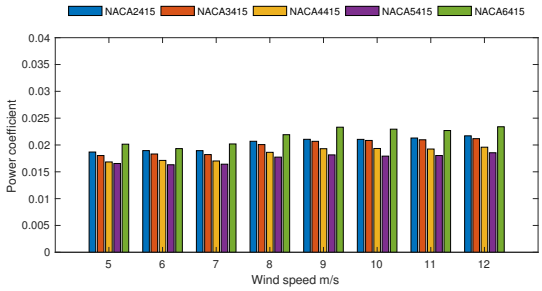

Figure 6. Power coefficients at a various wind speeds for different airfoil camber.

Influence of axial distance

Figure 7 shows the plot of C_p versus wind speed for NACA0015, for different axial distances (the distance between the top and bottom rotor). Note that for brevity we have not included the other airfoils (i.e. NACA0005, 0010, 0020, and 0025). The plot shows that the C_p is higher when the rotor dis-

tance is shorter. Furthermore, the closer rotor cases tend to have a higher rate of increase in C_p than that of larger distances. A similar trend has been reported by Didane et. al [4], where the C_p is greater when both rotors are in close proximity. Unlike HAWT, the VAWT rotors are located upper and lower of each other, not at the downwind location. Hence the VAWT would be less likely to suffer from undesirable vortex shedding from upstream turbines compared to HAWT. Furthermore, both of the VAWT rotors would receive the same amount of force from the incoming wind, hence we would expect that there would not be significant differences in C_p due to vertical distance between the two turbines. However, this is not the case as shown by our simulation results and that of Didane et. al [4]. It seems that the wingtip vortices from the upper or lower airfoils (or rotors) induce a higher lift force for the opposite airfoils.

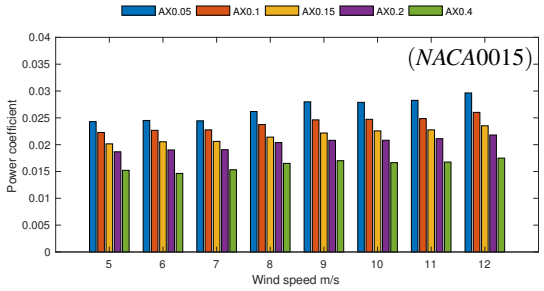

Figure 7. Power coefficients at a various wind speeds for different axial distance with NACA0015 airfoil.

Unlike the constant camber airfoil NACA0005, the NACA2415 exhibit a very different trend in C_p as the axial distance is increased. There is no clear trend between the five different axial distances. In fact, for NACA2415, the shortest axial distance produces the highest C_p. A similar inconsistency is also observed with the other different camber airfoil cases. It seems that the camber shape a dramatical influence on the wingtip vortex such that in certain cases it may no longer provide an additional lift force to the bottom rotor or vice versa. Hence one would need to carefully choose the proper airfoil profile to obtain the optimum C_p.

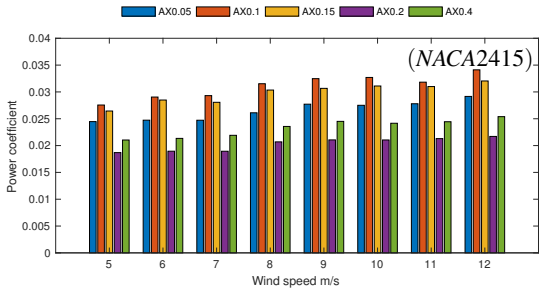

Figure 8. Power coefficients at a various wind speeds for different axial distance with NACA2415 airfoil.

Discussion

We have noticed that the C_p from our result are lower compared to that of Didane et al. [4]. This is due to the removal of the PVC tube in our simulation, which Didane et al [4] added to start the turbine. Even though the power coefficient decreased significantly without the PVC tube, both results demonstrate a similar trend after normalization relative to the power coefficient at maximum wind speed of 12 m/s (Figure 9). Moreover, the TSR range we used in our simulation is lower compared with other single rotor wind turbine (SRWT) study. The reason is to match the experiments performed by Didane et al. [4], as it is the only data we found for contra-rotating vertical axis wind turbine (CR-VAWT).

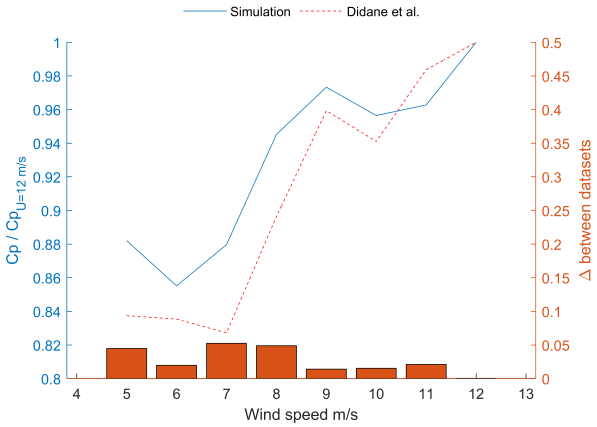

Figure 9. Simulation domain in (a) orthogonal view and (b) top view. Red region in (a) denotes rotating domain and the grey is stationary domain.

Conclusion

In this report, we have demonstrated the use of RANS to simulate a novel contra-rotating concept of an H-Darrieus type VAWT and investigated the effects of airfoil shape (both in thickness and camber) and axial distance on the turbine's coefficient of power. For the different airfoil thickness cases, the results show that a thicker airfoil would generate a higher C_p than that of the thinner airfoils. For the different airfoil camber cases, the C_p trend behaves differently for the largest airfoil camber (NACA6415). It seems that this particular cambered airfoil generates wingtip vortices that affect the opposite rotors' torque. Finally, for the influence of the axial distance between upper and lower rotors, the results show that for the symmetrical airfoils, a shorter vertical distance would result in a higher C_p. We believe that this is caused by the wingtip vortices from the upper or lower airfoils that induce a higher lift force for the opposite airfoils. However, this is not the case for the cambered airfoil. There is no clear trend in C_p when the axial distance is increased. This situation may be caused by the wingtip vortices of the cambered airfoils disturbing the lifting force of the opposite airfoils. The results and hypothesis, however, is still preliminary, further analysis on the wingtip vortices of the airfoils is needed.

References

[1] Bianchini, A., Ferrara, G. and Ferrari, L. (2015). Design guidelines for H-Darrieus wind turbines: Optimization of the annual energy yield. *Energy Conversion and Management*, 89, 690-707.

[2] Bhutta, M. M. A., Hayat, N., Farooq, A. U., Ali, Z., Jamil, S. R., and Hussain, Z. (2012). Vertical axis wind turbine: A review of various configurations and design techniques. *Renewable and Sustainable Energy Reviews*, 16(4), 1926-1939.

[3] Didane, D. H., Rosly, N., Zulkafli, M. F., and Shamsudin, S. S. (2018). Performance evaluation of a novel vertical axis wind turbine with coaxial contra-rotating concept. *Renewable Energy*, 115, 353-361.

[4] Didane, D. H., Rosly, N., Zulkafli, M. F., and Shamsudin, S. S. (2018). Numerical investigation of a novel contra-rotating vertical axis wind turbine. *Sustainable Energy Technologies and Assessments*, 31, pp. 43-53. (DOI:10.1016/j.seta.2018.11.006).